Hall-Effect Measurements Probing the Degree of Charge-Carrier Delocalization in Solution-Processed Crystalline Molecular Semiconductors

Jui-Fen Chang,[1] Tomo Sakanoue,[1] Yoann Olivier,[2] Takafumi Uemura,[3] Marie-Beatrice Dufourg-Madec,[4] Stephen G. Yeates,[4] Jérôme Cornil,[2] Jun Takeya,[3] Alessandro Troisi,[5] and Henning Sirringhaus[1,*]

[1]*Cavendish Laboratory, University of Cambridge, Cambridge CB3 OHE, United Kingdom*
[2]*Laboratory for Chemistry of Novel Materials, University of Mons, Place du Parc 20, 7000 Mons, Belgium*
[3]*The Institute of Scientific and Industrial Research, Osaka University, Ibaraki, Osaka, 567-0047, Japan*
[4]*Organic Materials Innovation Centre, School of Chemistry, University of Manchester, Oxford Road, Manchester, M13 9PL, United Kingdom*
[5]*Department of Chemistry and Centre for Scientific Computing, University of Warwick, Coventry CV4 7AL, United Kingdom*

(Received 23 December 2010; revised manuscript received 25 May 2011; published 2 August 2011)

Intramolecular structure and intermolecular packing in crystalline molecular semiconductors should have profound effects on the charge-carrier wave function, but simple drift mobility measurements are not very sensitive to this. Here we show that differences in the Hall resistance of two soluble pentacene derivatives can be explained with different degrees of carrier delocalization being limited by thermal lattice fluctuations. A combination of Hall measurements, optical spectroscopy, and theoretical simulations provides a powerful probe of structure-property relationships at a molecular level.

DOI: 10.1103/PhysRevLett.107.066601 PACS numbers: 72.80.Le, 71.15.Pd, 72.20.My

There has been tremendous progress in discovering solution-processible molecular semiconductors that provide high charge-carrier mobilities above 1 $cm^2/V\,s$ for a range of electronic applications. However, there is still considerable controversy about the degree to which the carrier wave function is extended over neighboring molecules and how this is impacted by molecular structure. Intermolecular interactions in molecular crystals with transfer integrals $J \approx 100$ meV should give rise to formation of mesoscopically extended Bloch electrons on a time scale $\tau_b = \hbar/J \approx 10fs$. Diagonal electron-phonon coupling, mainly due to intramolecular modes, occurs on a time scale comparable to that for charge delocalization and should result in renormalization of the transfer integral and polaronic relaxation [1]. Intermolecular reorganization on a slower time scale of $\tau_p > 100fs$ leads to dynamic fluctuations of the transfer integrals [2] and polarization energy [1]. These have been predicted to limit the length scale for charge delocalization to a few nm's, but experimental verification of this prediction is still missing.

Hall measurements should be a sensitive probe of the degree of charge delocalization as an ideal, free-electron Hall signature with Hall resistance, R_H, equal to the inverse charge concentration requires the charges to be at least partially extended over neighboring molecules to have a defined wave vector which can couple to the magnetic field through a Lorentz force equation [3]. Some molecular single crystals, such as rubrene [4], and polycrystalline films [5] exhibit free-electron Hall effects while other materials with similarly high drift mobilities, such as unsubstituted pentacene, deviate from ideal behavior. How such different signatures are related to molecular structure and packing is not well understood. Here we use Hall measurements combined with optical spectroscopy of charges and theoretical simulations to investigate the interplay between molecular structure and charge delocalization in polycrystalline films of two solution-processible pentacene derivatives, 6,13-bistriisopropyl-silylethynyl pentacene (TIPS-P) [6] and 1,4,8,11-tetramethyl-6,13-triethylsilylethynyl pentacene (TMTES-P) [7] [Fig. 1(a)].

Both molecules are oriented edge-on [6], but TIPS-P adopts *two-dimensional*, cofacial π stacking in the film plane, while TMTES-P exhibits *one-dimensional*, cofacial π stacking [6,7] (Fig. 1(a), Fig. S2 in the Supplemental Material [8]). Devices are fabricated in a top-gate field-effect transistor (FET) configuration with gold source-drain electrodes, TIPS-P and TMTES-P films spin coated from tetralin, a low-k Cytop gate dielectric and aluminum gate electrodes (Fig. S1(a) in [8]). Films of both materials are polycrystalline (Fig. S2(c) in [8]) [9]. For TIPS-P a field-effect mobility, $\mu_{\mathrm{FET}} = 2.1\ cm^2/V\,s$, was obtained [Fig. 1(b)]. For TMTES-P, we extracted slightly higher mobility of 2.6 and 3.5 $cm^2/V\,s$ above and below $V_g = -40$ V. Hall measurements in solution-processed organic semiconductors are challenging due to low mobility, high contact resistance and threshold voltage instabilities and to the best of our knowledge have not been reported before. We used a photolithographic technique for accurate, micrometer-scale patterning without device degradation [10] to shape the organic semiconductor into a Hall bar [Fig. 1(c)]. The sign of R_H is positive in both materials, consistent with operation in p-type accumulation mode. $1/R_H$ increases monotonically with $|V_g - V_{\mathrm{th}}|$ [Fig. 1(c)]. In TIPS-P, $1/R_H$ is about 2 times larger than the gate-induced charge density $Q \equiv C_i(V_g - V_{\mathrm{th}})$, similar to the behavior reported for vacuum-sublimed pentacene [11].

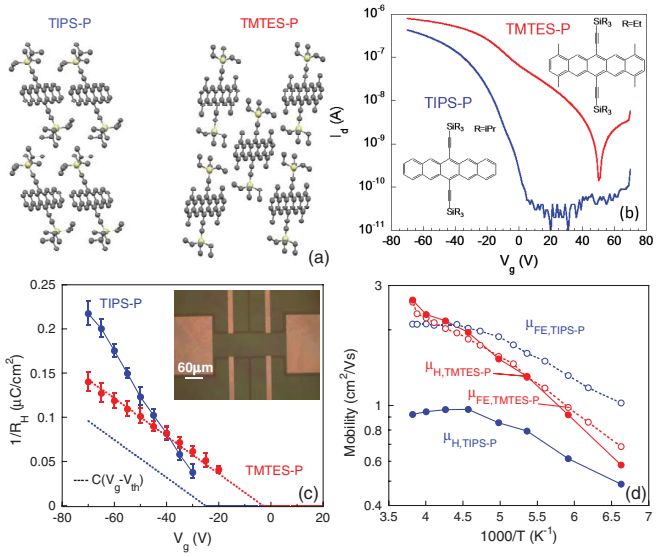

FIG. 1 (color). (a) Single-crystal structure of TIPS-P and TMTES-P viewed along the a axis. The one- and two-dimensional stacking of molecules can clearly be seen (Crystal structures from Refs. [6,7]). (b) Transfer characteristics of TIPS-P and TMTES-P Hall-bar FETs ($V_{ds} = -10$ V); (inset) molecular structures. (c) Inverse Hall coefficient $1/R_H$ and gate-induced charge density $Q \equiv C_i(V_g - V_{th})$ as a function of gate voltage at room temperature; (inset) optical image of TIPS-P Hall-bar FET. (d) Temperature dependence of Hall and field-effect mobilities ($V_g = -70$ V).

The Hall mobility, μ_H, is about half the field-effect mobility, μ_{FET}, from room temperature (RT) to 150 K [Fig. 1(d)]. Below 150 K the signal-to-noise ratio becomes too small for reliable Hall measurements. In contrast, TMTES-P exhibits a remarkably ideal Hall effect from RT to 150 K with $1/R_H$ coinciding with Q for $|V_g| > 20$ V and $\mu_{H=}\mu_{FET}$. In both materials μ_{FET} exhibits weakly temperature dependent transport between RT and 250 K. At lower temperatures the mobility becomes thermally activated with small activation energies of 30 meV (TIPS-P) and 40 meV (TMTES-P). This is consistent with the low electric field regime recently reported for TIPS-P [9]. In the long-channel Hall bars we cannot access the large field regime in which we observed a bandlike temperature dependence of the mobility.

A free-electron Hall signature is often interpreted simply in terms of the existence of mesoscopically extended Bloch electrons [4]. However, this is inconsistent with the charges' optical response as detected by charge modulation spectroscopy (CMS) and a more subtle interpretation is required. Charges in organic semiconductors have characteristic charge-induced optical absorptions, which differ from those of neutral molecules and reflect the degree of polaronic reorganization associated with charge formation. For TIPS-P FETs we previously reported two charge-induced absorption bands ($\Delta T/T < 0$) around 1.2 eV and 2.6 eV and an associated bleaching signal ($\Delta T/T > 0$)

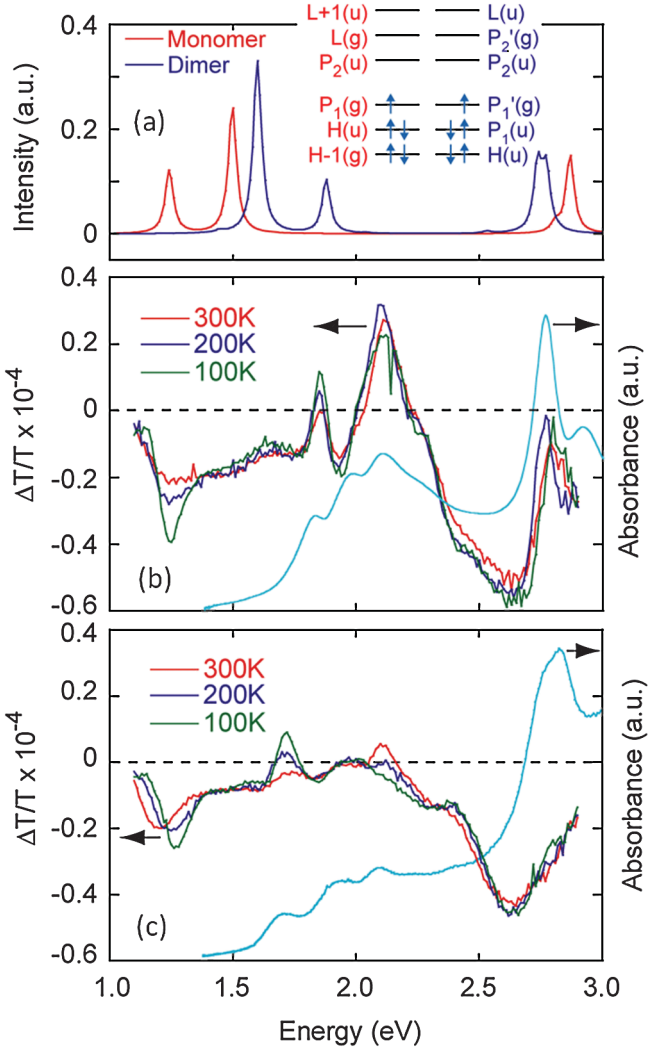

FIG. 2 (color). (a) Quantum-chemical simulation of the absorption spectrum of TIPS-P radical cation monomer (red) and dimer (blue) including energy level diagram; Temperature dependent differential transmission CMS spectra of TIPS-P (b) and TMTES-P (c) FETs. The thin film absorption spectra are shown as light blue curves.

of the neutral molecule absorption around 1.8–2.2 eV [Fig. 2(b)] [9]. To identify these transitions we have performed quantum-chemical calculations at semiempirical AM1 level with full configuration interaction (FCI) on an isolated TIPS-P monomer and a dimer (Fig. S3 in [8]). For the monomer radical cation they predict a first transition at 1.24 eV, primarily due to $P_1 \rightarrow P_2$, a second transition at 1.50 eV, primarily due to $H \rightarrow P_1$, and a higher energy transition at 2.8 eV, with its main oscillator strength from $P_1 \rightarrow L + 1$ [Fig. 2(a)]. Taking into account typical errors in estimating transition energies by gas-phase quantum-chemical computations, the theoretical monomer spectrum is in good agreement with the sharp low temperature CMS spectrum of TIPS-P, where charges are confined to isolated molecules in shallow trap states [9]. The sharp transition at

1.2 eV is most likely due to $H \rightarrow P_1$, while the $P_1 \rightarrow P_2$ transition is outside the experimental spectral range, but is observed at 1.0 eV in cationic TIPS-P in solution. For the dimer the charge is predicted to be fully delocalized over the two molecules with the lowest energy charge-induced absorptions blue shifted to 1.6 eV ($H \rightarrow P_1'$) and 1.88 eV ($P_1 \rightarrow P_2'$) and the higher energy transition slightly redshifted to 2.7 eV ($P_1 \rightarrow P_2'$). The differences in the monomer and dimer cation spectra suggest that the broad spectral features in the RT CMS spectrum of TIPS-P might be explained as an ensemble average over charges delocalized over different numbers $N = 2, 3, \ldots$ of molecules. The good agreement of the experimental CMS spectrum with the calculations on small molecular clusters implies that charges in TIPS-P are in fact not mesoscopically extended over 100's or 1000's of molecules, but only over a small number of molecules. For mesoscopically extended states new ''interband'' absorptions upon charge injection, such as $H \rightarrow P_1$, are still expected, but reorganization would be significantly reduced [12] and any transition from partially occupied to unoccupied levels, such as $P_1 \rightarrow P_2'$, at 2.6 eV should appear at energies close to those of the neutral molecule and not result in induced absorption.

TMTES-P exhibits similar charge-induced absorptions with similar optical cross section $\gamma = 1.4 \times 10^{-16}$ cm^2 for the transition near 2.6 eV [Fig. 2(c), $\gamma = 1.6 \times 10^{-16}$ cm^2 for TIPS-P]. The main difference is that in TMTES-P we detect no net bleaching signal ($\Delta T/T > 0$) at 300 K, although three vibronic peaks at 1.72 eV, 1.97 eV and 2.11 eV close to those in the thin film absorption spectrum are observed. Only at 100 K is there a small net bleaching signal (for a discussion of this effect, see [8]). We also performed CMS on rubrene single-crystal FETs with mobilities >5 cm^2/V s (Fig. 3). The rubrene CMS spectra are qualitatively similar to TMTES-P, with low-energy charge-induced absorption at 1.6 eV and higher-lying transition at 2.8 eV and similar absence of net bleaching. Since TMTES-P and rubrene [4] exhibit an ideal Hall effect to which *all* charges must contribute, we arrive at the important conclusion that an ideal Hall effect can arise in molecular systems, in which essentially none of the charges are mesoscopically extended, but charges are only delocalized over a small number of molecules.

To understand the difference in Hall signature we have applied a molecular model in which charge delocalization is limited by thermal lattice fluctuations [2]. For sufficiently small polaron binding energy E_b (~ 45 meV for pentacene) the main origin of carrier localization is not small polaron formation, but dynamic disorder or fluctuations in the hopping integrals. These have been calculated for the two molecules using combined molecular dynamics and quantum-chemical calculations [13]. For TIPS-P the average hopping integral V and standard deviation σ due to thermal fluctuations for pairs of molecules along the a and

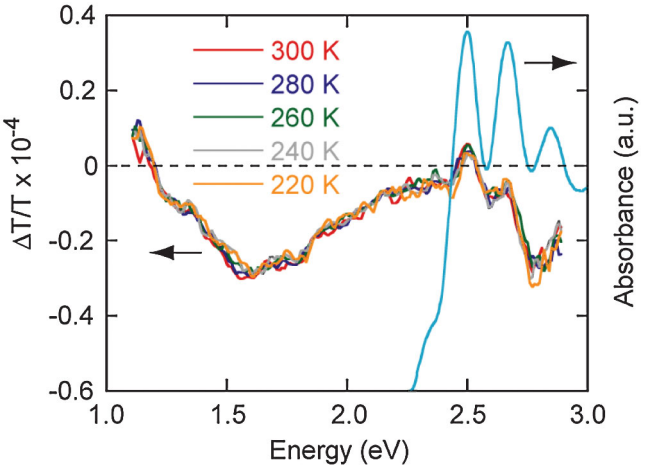

FIG. 3 (color). Temperature dependent differential transmission CMS spectrum of rubrene single-crystal FET with top-gate architecture and parylene gate dielectric. The spectra are independent of temperature down to 220 K, below which we encountered problems with irreversible device degradation due to thermal stress. The absorption spectrum of rubrene is shown as a light blue curve.

a-b crystal direction are $V_a = 64$ cm^{-1}, $\sigma_a = 342$ cm^{-1}, $V_{a-b} = 93$ cm^{-1}, $\sigma_{a-b} = 194$ cm^{-1}. For TMTES-P we find $V_a = 1646$ cm^{-1}, $\sigma_a = 444$ cm^{-1}, $V_b = -17$ cm^{-1}, $\sigma_b = 31$ cm^{-1}, i.e., the system is quasi-one-dimensional with large coupling along the a direction, in agreement with the crystal structure [Fig. 1(a)]. These data and the computed E_b can be mapped into a model Hamiltonian to study numerically the density of states (DOS) and the time evolution and localization length of the carrier wave function [8]. The computed isotropic mobilities of 5.1 and 12.4 cm^2 V^{-1} s^{-1} for TIPS-P and TMTES-P, respectively, are in a similar ratio as found experimentally for the Hall mobilities and close to the experimental values in absolute terms. For both molecules, there is substantial DOS broadening due to thermal motions. Within few k_BT from the DOS edge, the states are localized within a few molecules and this provides an explanation for observing the signature of localized states in CMS. However, the DOS shape for the two molecules is different. TMTES-P has a quasi-one-dimensional dispersion and smaller broadening due to a smaller fluctuation of the coupling [Figs. 4(a) and 4(b)]. When integrating the DOS to a charge concentration of 10^{19} cm^{-3} typical for the FET accumulation layer, the Fermi level is in a region with larger localization length for TMTES-P (> 10 Å) than for TIPS-P ($< 5 - 10$ Å). The Hall effect is expected to be sensitive to the degree of charge delocalization and existence of a nonzero wave vector and carrier momentum [3]. We verified that charges described by the model can indeed experience the Lorentz force. In the dynamic disorder model carriers undergo frequent scattering events approximately at each molecular site. However, the momentum expectation

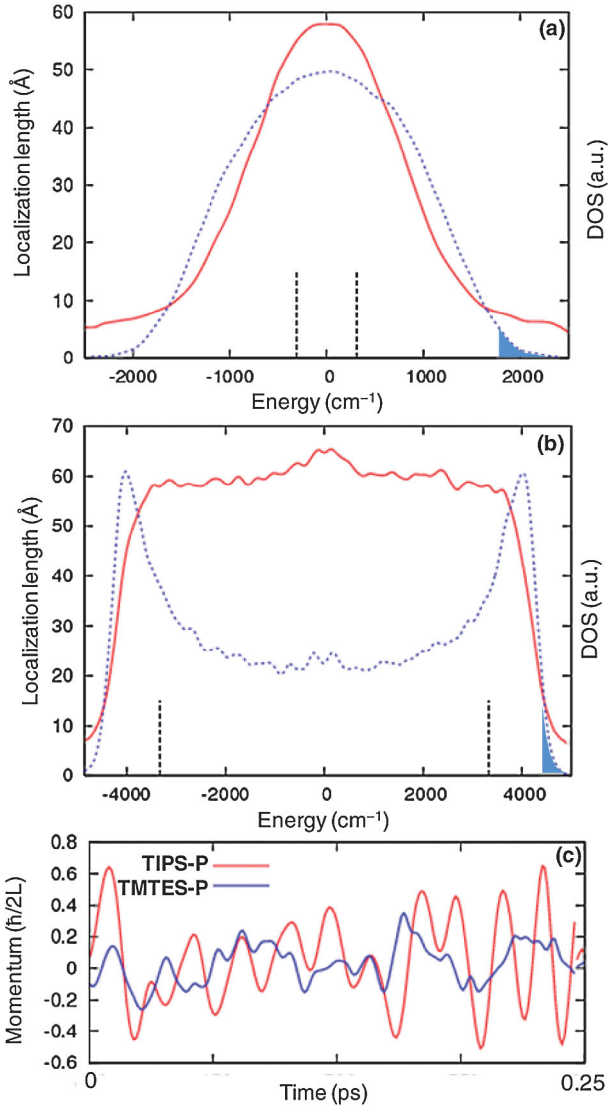

FIG. 4 (color). Localization length (red solid line) and DOS (blue dotted line) for TIPS-P (a) and TMTES-P (b). The vertical dashed lines represent the bandwidth in the absence of dynamic disorder. The light blue shaded area indicates the portion of the DOS which is expected to be occupied for a carrier concentration of 10^{19} cm^{-3}. (c) Oscillation of the expectation value of the linear momentum computed for a 1D model system of the two molecules.

value, $p_x(t) = \langle \psi(t)|\hat{p}_x|\psi(t)\rangle$, computed within the same model is indeed nonzero, though it oscillates strongly, as expected for coherent motion on the time scale of molecular vibrations [Fig. 4(c)]. This transport regime is similar to that of bad metals with weak electron correlation effects, where R_H remains ideal when the scattering length approaches the interatomic distance [14]. While there is no qualitative difference in the transport regime of the two materials, i.e., in both systems charges are not mesoscopically extended, the localization length of TMTES-P is evidently long enough that the majority of charges experience a semiclassical Lorentz force while in TIPS-P a significant portion of charges remain too strongly localized to contribute to an ideal Hall voltage. This model provides an explanation why depending on crystal structure some organic semiconductors exhibit an ideal Hall effect, while others with similar drift mobilities do not. In contrast to previous reports [15] we show that for some acenes 1D π stacking can result in excellent charge transport, but we caution that the difference between the two molecules investigated here might not extend to general rules about dynamic disorder in 1D and 2D conjugated systems. For any system a combination of Hall measurements, CMS, and theoretical simulations provides a powerful probe of charge delocalization as influenced by molecular structure.

We gratefully acknowledge funding from the Engineering and Physical Sciences Research Council and the Technology Strategy Board and helpful discussions with N. Cooper and P. Littlewood. J. C. and Y. O. received financial support from the Belgian National Fund for Scientific Research.

*hs220@cam.ac.uk

[1] J. D. Picon, M. N. Bussac, and L. Zuppiroli, Phys. Rev. B **75**, 235106 (2007).
[2] A. Troisi and G. Orlandi, Phys. Rev. Lett. **96**, 086601 (2006).
[3] H. Fukuyama, H. Ebisawa, and Y. Wada, Prog. Theor. Phys. **42**, 494 (1969).
[4] V. Podzorov, E. Menard, J. A. Rogers, and M. E. Gershenson, Phys. Rev. Lett. **95**, 226601 (2005).
[5] M. Yamagishi, J. Soeda, T. Uemura, Y. Okada, Y. Takatsuki, T. Nishikawa, Y. Nakazawa, I. Doi, K. Takimiya, and J. Takeya, Phys. Rev. B **81**, 161306(R) (2010).
[6] J. E. Anthony, J. S. Brooks, D. L. Eaton, and S. R. Parkin, J. Am. Chem. Soc. **123**, 9482 (2001).
[7] G. R. Llorente, M. B. Dufourg-Madec, D. J. Crouch, R. G. Pritchard, S. Ogier, and S. G. Yeates, Chem. Commun. (Cambridge) **21**, 3059 (2009).
[8] See Supplemental Material at http://link.aps.org/supplemental/10.1103/PhysRevLett.107.066601 for details of the experimental setup, crystal structures, and theoretical model.
[9] T. Sakanoue and H. Sirringhaus, Nature Mater. **9**, 736 (2010).
[10] J. F. Chang, M. C. Gwinner, M. Caironi, T. Sakanoue, and H. Sirringhaus, Adv. Funct. Mater. **20**, 2825 (2010).
[11] T. Sekitani, Y. Takamatsu, S. Nakano, T. Sakurai, and T. Someya, Appl. Phys. Lett. **88**, 253508 (2006).
[12] S. T. Bromley, F. Illas, and M. Mas-Torrent, Phys. Chem. Chem. Phys. **10**, 121 (2008).
[13] A. Troisi, Adv. Mater. **19**, 2000 (2007).
[14] P. H. Dai, Y. Z. Zhang, and M. P. Sarachik, Phys. Rev. Lett. **70**, 1968 (1993).
[15] J. E. Anthony and B. Purushothaman, in *Organic Field-Effect Transistors Vi*, edited by Z. Bao and D. J. Gundlach (Spie-Int Soc Optical Engineering, Bellingham, 2007), Vol. 6658, pp. L6580-L6580.